Spin-Dependent Electron Dynamics in Front of a Ferromagnetic Surface

Anke B. Schmidt,[1,*] Martin Pickel,[2] Martin Wiemhöfer,[2] Markus Donath,[2] and Martin Weinelt[1,3]

[1]*Max-Born-Institut, Max-Born-Str. 2A, 12489 Berlin, Germany*

[2]*Physikalisches Institut, Westfälische Wilhelms-Universität Münster, Wilhelm-Klemm-Str. 10, 48149 Münster, Germany*

[3]*Freie Universität Berlin, Fachbereich Physik, Arnimallee 14, 14195 Berlin, Germany*

(Received 28 January 2005; published 2 September 2005)

Exchange splitting and dynamics of image-potential states in front of a 3 monolayer iron film on Cu(100) have been studied with time-, energy-, and spin-resolved bichromatic two-photon photoemission. For the first image-potential state $n = 1$ we observe an exchange splitting of 56 ± 10 meV and spin-dependent lifetimes of 16 ± 2 fs for majority-spin and of 11 ± 2 fs for minority-spin electrons, respectively. The time-resolved studies of both the population and the linewidth of image-potential states manifest that at the magnetic surface not only inelastic but also quasielastic scattering processes are spin dependent.

DOI: 10.1103/PhysRevLett.95.107402 PACS numbers: 78.47.+p, 73.20.At, 75.70.Ak, 79.60.Dp

Recent experiments demonstrate that significant demagnetization of ferromagnetic thin films upon laser excitation can be achieved within a few hundred femtoseconds [1–4]. Within this time scale the excited electronic system and the underlying lattice are not in equilibrium [1] and it seems that the transient hot electron population is responsible for the change of the magnetization [5,6]. Which processes lead to the loss of magnetization remains controversial. Studying ultrafast spin-dependent electron dynamics is therefore essential to understand which processes may have a part in magnetization reversal processes on the femtosecond time scale [7,8]. For a technological application of this ultrafast demagnetization phenomenon, e.g., in laser assisted recording of hard disks, a thorough understanding of all aspects involved is required. The modeling of the fundamental demagnetization process is still in its infancy and asks for experiments on simple, well-defined model systems which give access to a microscopic description of spin-dependent electron scattering processes.

Such systems are image-potential states [9], the dynamics of which can be studied with femtosecond time resolution by two-photon photoemission (2PPE) [10–13]. An electron excited by a first laser pulse is trapped in the image potential at a few Ångstrom distance in front of the surface. The weak coupling to bulk states leads to lifetimes of tens of femtoseconds [9,10] and the evolution of the transient population can be sampled by a second time-delayed probe pulse [14]. This allows us to quantify inelastic scattering processes which always lead to a decay of the population. Quasielastic scattering events in contrast may only destroy the phase coherence. For the well-defined image-potential states these dephasing rates can be identified by analyzing the delay-dependent linewidth [15]. On ferromagnetic surfaces the image-potential states are expected to reflect the exchange-split bulk-band gap boundaries and should thus allow us to study spin-dependent relaxation processes directly in the time domain. Comprehensive studies of surface electronic states, including image-potential states, have been performed on low-index surfaces of ferromagnets [16]. The surface-state appearance at ferromagnetic surfaces is much more complex than at noble metal surfaces, due to the presence of the magnetic d states [17]. This is true for the image-potential states as well but they are still well separated from other states and clearly detectable. Spin-resolved inverse-photoemission data for the $n = 1$ image-potential states at ferromagnets reveal spin-dependent binding-energy differences between 20 and 80 meV and spin-dependent linewidths have been observed for Fe(110) [18,19]. These results are supported by polarization-dependent two-photon photoemission experiments for Fe films on Cu(100) and W(110) [20]. Nevertheless, all of these experiments suffer from either long data-acquisition times at moderate energy resolution or the lack of spin resolution, and no measurements of a spin-dependent lifetime in the time domain and of the pure dephasing rates have been performed yet.

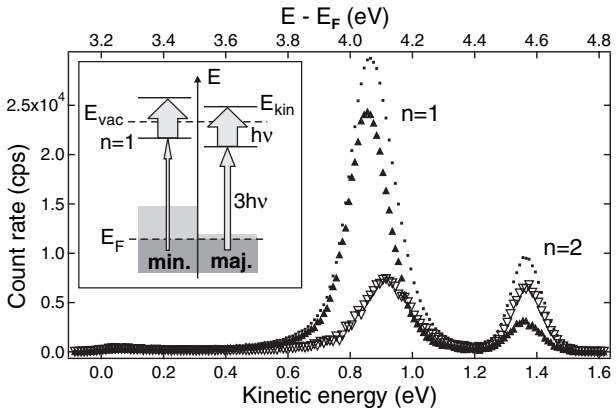

FIG. 1. Energy-resolved 2PPE spectra at zero time delay between pump and probe pulse, spin integrated (•) and spin resolved; the exchange splitting between the majority (▲) and minority (▽) components is clearly discernible. A schematic representation of bichromatic 2PPE is shown in the inset.

In this Letter we show by a combination of time-, energy-, and spin-resolved 2PPE that not only the lifetime but also the pure dephasing rate differ for majority-spin and minority-spin image-potential states. Therefore, both inelastic and quasielastic scattering processes at the iron thin film surface are spin dependent. In the experiment we use the frequency-tripled radiation from a Ti:sapphire oscillator as pump pulse to excite electrons from the valence band into the image-potential state. The fundamental ($h\nu = 1.56$ eV) of the oscillator serves as probe pulse to raise the excited electrons above the vacuum energy (cf. inset in Fig. 1). Pulse widths were 57 fs and 42 fs, respectively. The photoelectrons are selected by energy using a 300 mm cylindrical mirror analyzer (FOCUS GmbH). Energy and angular resolution are 65 meV and accordingly $\pm 2.5°$. Spin resolution is achieved by spin-polarized low-energy electron diffraction (SP-LEED) at a W(100) crystal [21].

Figure 1 shows energy-resolved 2PPE spectra for 3.0 ± 0.2 ML (monolayer) Fe on Cu(100). Coverage was controlled by recording the medium-energy electron diffraction intensity oscillations during evaporation, which indicate smooth layer-by-layer growth after the first two monolayers, and by the characteristic LEED patterns after evaporation [22]. The iron films were deposited at room temperature at a rate of 0.3 ML per minute. 3 ML iron on copper is ferromagnetic with the easy magnetization direction normal to the surface [22]. The geometric structure of the films has been described as a shear-deformed fcc structure or shear-deformed bcc(110)-like surface, heavily strained, in any case, to match the fcc(100) substrate [23,24].

2PPE spectra are recorded in normal emission for p-polarized laser pulses and at a sample temperature of 90 K. The data in Fig. 1 stem from two averaged data sets obtained at reversed perpendicular magnetization of the film, thereby eliminating a slight instrumental asymmetry of 10% between (20) and $(\bar{2}0)$ SP-LEED spots. The individual contribution of majority and minority channels in Fig. 1 were evaluated using a Sherman function of $S = 0.22 \pm 0.02$ for the spin-polarization detector. This value and the corresponding error was determined assuming that the exchange splitting of the first image-potential state is the same for excitation with p- and s-polarized light (the ratio of majority to minority intensities depends strongly on the polarization of the exciting light). S is thus in the expected range of $S = 0.19 \ldots 0.28$ [21]. We find an exchange splitting of 56 ± 10 meV for the $n = 1$ image-potential state with the error dominated by the uncertainty in S. For the $n = 2$ image-potential state an exchange splitting of 7 ± 3 meV was observed. The bulk penetration of the image-potential states decreases $\propto n^{-3}$. The observed n dependence thus confirms that the spin splitting of the image-potential states reflects the exchange-split bulk-band-gap boundaries weighted by the bulk penetration ($7 \text{ meV}/2^{-3} = 56$ meV).

Assuming that a simple band structure for exchange-split bulk fcc-iron [25] describes the initial states well enough, the different intensities of the majority and minority components in the $n = 1$ and the $n = 2$ image-potential states may be interpreted in terms of the excitation conditions from bulk states. Symmetry considerations and dipole-selection rules determine that excitation into image-potential states at $k_{\parallel} = 0$ in front of an fcc(100) surface with p-polarized light may occur from Δ_1 and Δ_5 states [26]. Additionally, the transition matrix element is largest for initial states near the X point and accounts for the strength of the excitation process from the bulk states along ΓX of the fcc Brillouin zone into the image-potential states [27]. With this, the observed spin-dependent intensities in the $n = 1$ and $n = 2$ image-potential states can be explained qualitatively. A quantitative agreement is not to be expected as the structure of ultrathin iron films on copper is far from the ideal pseudomorph. It becomes clear from these considerations that spin-resolved 2PPE measurements have a high band structure sensitivity. With a variation of the energy and polarization of the pump and probe pulses, these measurements may contribute to a confirmation and refinement of previous band structure models for thin magnetic films.

Considering the substantial loss of about 4 orders of magnitude, which the spin-resolving detection scheme involves, the count rate per second is nevertheless sufficient for time-dependent measurements. Evidence for spin-dependent lifetimes may be viewed from the energy-resolved data in Fig. 2(a). With increasing delay between pump and probe pulses the minority intensity drops faster compared with the majority channel. Note that the spectra are normalized to equal majority intensity.

For the time-resolved measurements in Fig. 2(b) the energy of the analyzer is held constant at the peak maximum of the respective spin channel while the intensity is recorded as a function of pump-probe delay. We employed shorter pulses of 30 fs for the time-resolved measurements. By comparison with the cross correlation of pump and probe pulse [taken from a measurement of the occupied Shockley surface state on Cu(111)] we directly see a spin-dependent broadening of the $n = 1$ trace [Fig. 2(b)] for positive delay. This is again a clear signature of a spin-dependent lifetime. A quantitative data analysis was done by a fit employing optical Bloch equations. This yields lifetimes of 16 ± 2 fs and 11 ± 2 fs for majority electrons and minority electrons, respectively, in the $n = 1$ image-potential state and of 47 ± 3 fs and 35 ± 3 fs in the $n = 2$ image-potential state. The longer lifetimes of the $n = 2$ state allow us to deduce its spin-dependent lifetimes directly from the exponential decay at delay times beyond the cross correlation [28]. Within error bars the ratio of minority versus majority lifetimes is independent of the quantum number n. The ratio of $n = 1$ to $n = 2$ lifetimes for each spin channel mirrors the ratio of the respective lifetimes measured, e.g., on Cu(100) [14].

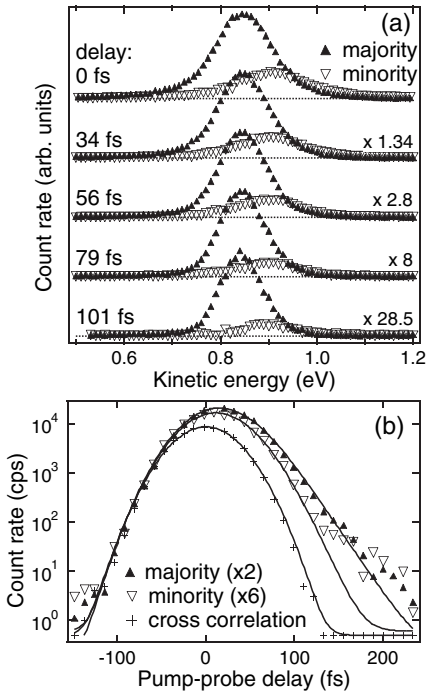

FIG. 2. (a) Energy- and spin-resolved 2PPE spectra of the $n = 1$ image-potential state for increasing pump-probe delay; the spectra are normalized on the spin-up channel at 0 fs; the numbers on the right indicate the multiplication factors of the intensity. (b) Time-resolved 2PPE spectrum of the $n = 1$ image-potential state for majority (▲) and minority (▽) electrons and the cross correlation between pump and probe pulses (+). The fit (solid lines) was done employing Bloch equations.

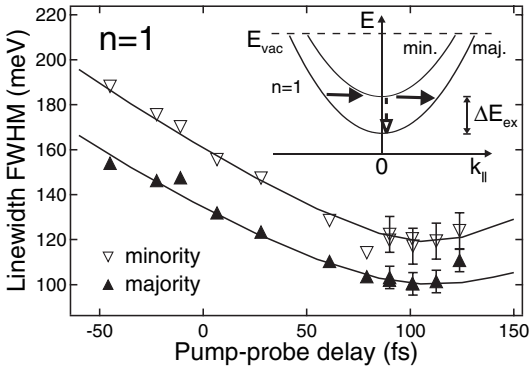

FIG. 3. Measured (symbols) and calculated (solid lines) linewidths of the majority (▲) and minority (▽) components of the first image-potential state as a function of pump-probe delay. Where the experimental uncertainty exceeds the symbol size error bars are indicated. In the inset the dispersing image-potential bands are shown schematically and possible elastic and inelastic scattering processes are indicated.

While inelastic scattering (and quasielastic scattering into bulk states) diminishes the population of the excited states, i.e., governs the lifetime, quasielastic scattering within the image-potential-state bands destroys the phase relation between the electron wave function and the laser field. This is described by the so-called dephasing time, a concept similar to the decoherence time (or transversal relaxation time) T_2 known from the Bloch equations for spin ensembles. Both the decay and dephasing independently contribute to the linewidth of the intermediate state in 2PPE.

A closer look at the spectra in Fig. 2(a) reveals that the linewidth of the $n = 1$ image-potential state depends on pump-probe delay. Corresponding data for the majority and minority electrons may be viewed in Fig. 3. The linewidth versus pump-probe delay has been analyzed using three-level optical Bloch equations (solid lines in Fig. 3) [15]. Simplistically, the observed dependence may be understood in terms of the following three considerations. First, at significant negative delay, the probe pulse precedes the pump pulse and photoemission is mainly caused by the time-overlapping tails of pump and probe pulse. This seemingly narrows the pulse duration which corresponds to a broadening in the frequency domain. Evidently, the increase of the linewidth with increasing negative pump-probe delay depends on both pulse shape and duration. The modeling of the data shows that the linear increase observed in Fig. 3 is a signature of Gaussian shaped laser pulses [15]. Second, for a constant population of the intermediate state $P(t) = \text{const}$ (which could be realized by cw excitation, for example), ionization of the intermediate state by the probe pulse corresponds to conventional photoemission. From photoemission it is well known that the linewidth is given by $\Gamma = \hbar/\tau + 2\Gamma^*$, where τ is the intermediate state lifetime and Γ^* the so-called (pure) dephasing rate ($\Gamma^* = \hbar/T_2$). For excitation with a femtosecond laser pulse the balance of population buildup and decay holds for one particular delay only, where $dP(t)/dt = 0$. However, it is comprehensible that as long as the pump pulse is active, both lifetime and dephasing contribute to the linewidth. Third, when the pump pulse is over, the population simply decays exponentially $P(t) \propto \exp(-t/\tau)$. Without dephasing, the photoemission signal equals a convolution of the Gaussian probe pulse with an exponential function. This yields a Gaussian, shifted, but not broadened. Thus at large delay only the dephasing rate $2\Gamma^*$ but not the lifetime contributes to the measured linewidth. Moreover, when the pump pulse is over, details of the excitation process such as the density of initial states do not influence the measured linewidth. Hence we are provided with an excellent possibility to measure the dephasing rate. As the probe pulse (and of course, the experimental resolution) is identical for majority and minority electrons, the difference in linewidths for a high pump-probe delay clearly suggests spin-dependent dephasing.

For the simulation (solid lines in Fig. 3), the pulse lengths have been determined from interferometric autocorrelation and cross-correlation measurements from the

occupied surface state on Cu(111). A reconstruction of the pulses from the autocorrelation confirmed the Gaussian shaped envelope of our probe pulse. Also, the lifetimes have been independently gathered from the time-resolved 2PPE spectra. Hence only the dephasing rate remains to be derived from the simulation. The simulation employed a pure dephasing rate of 10 meV and 20 meV for majority- and minority-spin electrons, respectively [29]. From the conformance of the simulation with the measured data one can conclude that we observe spin-dependent quasielastic scattering processes. The increase in the linewidth for a pump-probe delay larger than 120 fs can be attributed to inelastic interband scattering from the $n = 2$ into the $n = 1$ image-potential state [30].

All of these findings demonstrate that both inelastic and quasielastic scattering and thus hot electron relaxation after laser excitation is spin dependent at ferromagnetic surfaces. It has been suggested previously [19,31] that the shorter *inelastic* lifetime of minority-spin electrons is due to the larger number of unoccupied states available for scattering into. This is unquestionably the case, but in addition to this we observe a large difference in the quasielastic scattering rate of spin-up and spin-down electrons. This leads to a spin-dependent decline in population as well, because the electrons may also scatter *elastically* into unoccupied bulk states, from where they can relax very fast towards the Fermi level.

In the inset of Fig. 3 the dispersing image-potential bands of the $n = 1$ state are shown schematically. A scattering process which might very well stand behind the quasielastic scattering processes discussed in the section about linewidth analysis is magnon emission and absorption. An acoustic spin wave in iron is of around 3 meV in energy for the necessary momentum transfer between the minority and majority band [32,33]. Magnon emission (minority into majority band) and magnon absorption (majority into minority) are illustrated with horizontal arrows. At a sample temperature of 100 K, both processes are comparable, thus conserving the population. The vertical arrow represents an inelastic scattering process within the $n = 1$ state with zero momentum transfer including a spin flip. This, however, would appear in the lifetime in spin-sensitive measurements, but not in the dephasing.

In conclusion, we have shown that image-potential states, accessible by spin-resolved 2PPE, provide a simple model system for a detailed investigation of spin-dependent electron dynamics directly in the time domain and the identification of spin-dependent scattering processes at surfaces. These findings will now allow us to investigate whether a certain fraction of the observed scattering processes indeed involve a spin flip and thus pinpoint one of the elementary steps made responsible for the loss of magnetization.

We thank Thomas Fauster for valuable discussions. Financial support by the Deutsche Forschungsgemeinschaft through the priority program *Ultrafast magnetization processes* is gratefully acknowledged.

*Electronic address: anke.schmidt@mbi-berlin.de

[1] E. Beaurepaire *et al.*, Phys. Rev. Lett. **76**, 4250 (1996).
[2] A. Scholl *et al.*, Phys. Rev. Lett. **79**, 5146 (1997).
[3] B. Koopmans *et al.*, Phys. Rev. Lett. **85**, 844 (2000).
[4] H.-S. Rhie, H. A. Dürr, and W. Eberhardt, Phys. Rev. Lett. **90**, 247201 (2003).
[5] J. Hohlfeld *et al.*, Phys. Rev. Lett. **78**, 4861 (1997).
[6] L. Guidoni, E. Beaurepaire, and J.-Y. Bigot, Phys. Rev. Lett. **89**, 017401 (2002).
[7] B. Koopmans, M. van Kampen, and W. J. M. Jonge, J. Phys. Condens. Matter **15**, S723 (2003).
[8] V. P. Zhukov, E. V. Chulkov, and P. M. Echenique, Phys. Rev. Lett. **93**, 096401 (2004).
[9] P. M. Echenique and J. B. Pendry, J. Phys. C **11**, 2065 (1978).
[10] U. Höfer *et al.*, Science **277**, 1480 (1997).
[11] M. Roth *et al.*, Phys. Rev. Lett. **88**, 096802 (2002).
[12] K. Boger, M. Weinelt, and Th. Fauster, Phys. Rev. Lett. **92**, 126803 (2004).
[13] P. M. Echenique *et al.*, Surf. Sci. Rep. **52**, 219 (2004).
[14] M. Weinelt, J. Phys. Condens. Matter **14**, R1099 (2002).
[15] K. Boger *et al.*, Phys. Rev. B **65**, 075104 (2002).
[16] M. Donath, Surf. Sci. Rep. **20**, 251 (1994).
[17] J. Braun and M. Donath, Europhys. Lett. **59**, 592 (2002).
[18] F. Passek and M. Donath, Phys. Rev. Lett. **69**, 1101 (1992).
[19] F. Passek *et al.*, Phys. Rev. Lett. **75**, 2746 (1995).
[20] U. Thomann *et al.*, Appl. Phys. B **68**, 531 (1999); Phys. Rev. B **61**, 16163 (2000).
[21] J. Kirschner and R. Feder, Phys. Rev. Lett. **42**, 1008 (1979).
[22] J. Thomassen *et al.*, Phys. Rev. Lett. **69**, 3831 (1992).
[23] L. Hammer, S. Müller, and K. Heinz, Surf. Sci. **569**, 1 (2004).
[24] A. Biedermann *et al.*, Appl. Phys. A **78**, 807 (2004).
[25] G. J. Mankey, R. F. Willis, and F. J. Himpsel, Phys. Rev. B **48**, 10284 (1993).
[26] W. Eberhardt and F. J. Himpsel, Phys. Rev. B **21**, 5572 (1980).
[27] W. Wallauer and Th. Fauster, Phys. Rev. B **54**, 5086 (1996).
[28] I. L. Shumay *et al.*, Phys. Rev. B **58**, 13974 (1998).
[29] Usually the corresponding rates are given in meV rather than s^{-1}, according to the relation $\Gamma = \hbar/\tau$.
[30] K. Boger, Th. Fauster, and M. Weinelt, New J. Phys. **7**, 110 (2005).
[31] M. Aeschlimann *et al.*, Phys. Rev. Lett. **79**, 5158 (1997).
[32] H. A. Mook and R. M. Nicklow, Phys. Rev. B **7**, 336 (1973).
[33] R. Vollmer *et al.*, Thin Solid Films **464**, 42 (2004).